Thin Solid Films 519 (2010) 1649–1654

Contents lists available at ScienceDirect

Thin Solid Films

journal homepage: www.elsevier.com/locate/tsf

In-situ X-ray diffraction studies of time and thickness dependence of crystallization of amorphous TiO_2 thin films and stress evolution

R. Kužel [a,*], L. Nichtová [a], Z. Matěj [a], J. Musil [b]

[a] Department of Condensed Matter Physics, Faculty of Mathematics and Physics, Charles University in Prague, 121 16 Praha 2, Czech Republic
[b] Department of Physics, Faculty of Applied Sciences, University of West Bohemia in Pilsen, Pilsen, Czech Republic

ARTICLE INFO

Available online 28 September 2010

ABSTRACT

Remarkable properties of titanium dioxide films such as hydrophilicity or photocatalytic activity depend largely on their phase composition, microstructure and in particular on the crystallinity. By in-situ X-ray diffraction studies of isochronal and isothermal annealing of amorphous films with different thickness at different temperatures it was found that the crystallization process can be quite well described by the Johnson-Mehl-Avrami-Kolmogorov formula modified by the introduction of crystallization onset. This and other parameters of the formula strongly depend on the film thickness. For thickness below about 500 nm the crystallization is very slow. Simultaneously, the appearance and increase of tensile stresses with the annealing time were observed and these stresses were confirmed by detailed studies by both total pattern fitting and $\sin^2\psi$ method on post-annealed samples. The stresses rapidly increase with decreasing thickness of the films. It seems that there is a strong correlation between the stresses and crystallization onset and/or crystallization rate. Tensile stresses that are generated during crystallization further inhibit crystallization and cause significant thickness dependence of the crystallization. The temperature and time dependence of microstructure of crystallized amorphous films differ significantly from those obtained for as-deposited nanocrystalline films or nanocrystalline powders. During annealing, quite large crystallites are formed quickly with the preferred orientation (001) that is suppressed with the proceeding time.

1. Introduction

Titanium dioxide is a well-known material that found numerous applications in different fields. It is the most widely used white pigment because of its brightness and very high refractive index. In the past years, higher attention has been devoted to thin films used as ultra thin film coatings, nanostructured membranes, in electrochemistry and electrocatalysis, in microoptics and electrooptics, medicine, cosmetics and in photocatalysis [1–4]. The applications depend significantly on the layer properties (stability, transparency, photoconductivity, photoactivity, etc.) and their microstructure (surface area, pore size distribution, particle size, crystallographic structure, and phase composition). The films can be prepared by several techniques, the sol–gel probably being most frequent but the magnetron deposition is favorable from the point of view of mechanical durability required for practical applications. Depending on the deposition conditions, the films can be prepared as amorphous or nanocrystalline. Completely amorphous films often do not have required properties (hydrophilicity, photocatalytic activity) and it seems that partially crystalline or nanocrystalline form is preferred. This can be achieved either by annealing of amorphous materials or by appropriate selection of deposition parameters. Nanocrystalline anatase is supposed to have higher photocatalytic activity than other titania phases [5].

In previous studies of microstructure evolution and crystallization in the post-annealed amorphous and nanocrystalline magnetron deposited films [6] we have found that the amorphous TiO_2 films can be crystallized at about 250 °C. The diffraction peaks were quite narrow and their crystallite size was estimated to be larger then 100 nm immediately after the onset of crystallization. However, the films with the thickness below 200 nm crystallized at higher temperatures (up 350 °C for the films below 100 nm). Texture was usually absent in these films except the thinnest ones where a weak (101) fiber texture was found. Tensile residual stresses have been found in all the crystallized films and relaxed after annealing at 500 °C. Studies of the deposited nanocrystalline films with different thickness [7] showed that rutile phase grows on the interface with the substrate and it is replaced with anatase with increasing distance from the substrate. This was confirmed by coplanar grazing incidence depth profiling. Therefore thinner nanocrystalline films contained mainly rutile while in thicker films anatase was dominating. The stresses in as-deposited nanocrystalline films were small (<100 MPa) but complicated (triaxial, possible gradients) and the texture was not always fiber and it was inclined with respect to the surface. This was

* Corresponding author.
E-mail address: kuzel@karlov.mff.cuni.cz (R. Kužel).

0040-6090/$ – see front matter © 2010 Elsevier B.V. All rights reserved.
doi:10.1016/j.tsf.2010.08.122

probably related to geometry of deposition (dual magnetron). Transformation of anatase into rutile started at about 700 °C.

In order to confirm thickness dependence of crystallization and study further the process, in-situ studies were performed here and the results of measurements on a set of titanium dioxide thin films with different thickness deposited on silicon substrate is presented. Both isochronal and isothermal annealing were performed.

Surprisingly, systematic studies of the film thickness dependence of crystallization are quite rare but they usually show an increase of the crystallization temperature with decreasing thickness (see for example Ref. [8] on $Sb_{70}Te_{30}$ films). However, the explanation of the effect is rather different in individual cases. For example the increase of crystallization temperature of amorphous $Ba_xSr_{1-x}TiO_3$ films to perovskite with the film thickness was attributed to the observed intermediate phase [9], while the explanation given for Ba–ferrite films is based on epitaxial growth [10] and thickness dependent interfacial energy is considered in Ref. [11]. Zhaom et al. [12] found not only that the crystallization onset is higher for thinner films but also that this effect depends on the material (HfO_2, ZrO_2). This even more stimulates more detailed studies of the process.

2. Experimental conditions

2.1. Sample preparation

Titanium dioxide films were prepared by sputtering with dual magnetron equipped with two Ti (99.5) targets of 50 mm in diameter and supplied by a dc-pulsed Advanced Energy Pinnacle Plus + 5 kW power supply unit operating in a bipolar asymmetric mode at repetition frequency $f_r = 100$ kHz and duty cycle $\tau/T = 0.5$; where τ and T are the length of pulse and the period of pulses. Films were deposited on unheated silicon (100) substrates (15 × 10 × 1 mm) at substrate to target distance $d_{s-t} = 100$ mm, total working pressure $p_T = 0.5$ Pa, average pulse discharge current $I_{da1,2} = 1.5$ A and average pulse power density $W_{da} \approx 20$ Wcm^{-2}. Further details on the dual magnetron system are given elsewhere [13].

Two identical sets of samples with different thicknesses of 48, 100, 130, 180, 300, 440, 630, and 800 nm were measured during isochronal and isothermal annealing, respectively.

2.2. XRD measurements

In-situ high-temperature measurements were performed in MRI high-temperature chamber with both radiant and direct heating. The films deposited on the Si substrate were fixed on the top of PtRh strip heater with a silver paste which is a way applicable for temperatures below about 700 °C. Temperature was measured by the thermocouple fixed to the bottom of the strip. Calibration of actual temperature on the film surface was performed by using of thin Al paste layer on the same substrates. Aluminum is suitable because of its high thermal expansion coefficient and consequently large XRD peak shifts even with small temperature changes. The films were heated primarily by radiant heater and the temperatures on their top was about 8–10 °C higher than the values measured by the thermocouple. The HT chamber was placed on the vertical Panalytical X'Pert Pro theta–theta goniometer. The parallel beam diffraction geometry consisted of parabolic Goebel mirror with slit and mask in the primary beam and parallel plate collimator and proportional point gas detector in the diffracted beam. The angle of incidence of 1° was used for all the 2θ scans of the in-situ HT measurements. Each time after setting the temperature, alignment of the specimen was checked by measurement of primary beam and specimen position was corrected if necessary in order to keep the irradiated area in the specimen center. The alignment took always less than 3 min which is important for isochronal annealing experiments.

Two anatase peaks – 101 and 004 – were analyzed only during the in-situ measurements. More detailed studies are under way. The peaks were fitted with the Pearson VII function and the peak positions, integrated intensities and integral breadths were determined. Total pattern fitting by the program MStruct was used for the evaluation of the whole diffraction patterns taken at room temperature. More details can be found in [14,15].

The room temperature measurements were performed on Panalytical X'Pert MRD horizontal diffractometer in a similar parallel beam setup, by the 2θ scans with the angle of incidence fixed at 0.5°. The measurements of residual stresses were also carried out by using a parallel beam setup but with a point focus and polycapillary instead of the Goebel mirror and by using the Eulerian cradle for the conventional sin²ψ method. Up to seven different peaks of anatase were analyzed and the stress values averaged.

3. Results

3.1. Isochronal annealing

In the first step, the results from post-annealed samples [6] were verified by the isochronal annealing experiments starting at 180 °C with a step of 20 °C up to 500 °C. The 101 anatase peak was measured and two subsequent scans (12 min each) were taken at each fixed temperature. The total time of the specimen at the temperature was 30 min. It was clearly shown again that the crystallization temperature for the thinner film is higher (example on Fig. 1). Actually there is

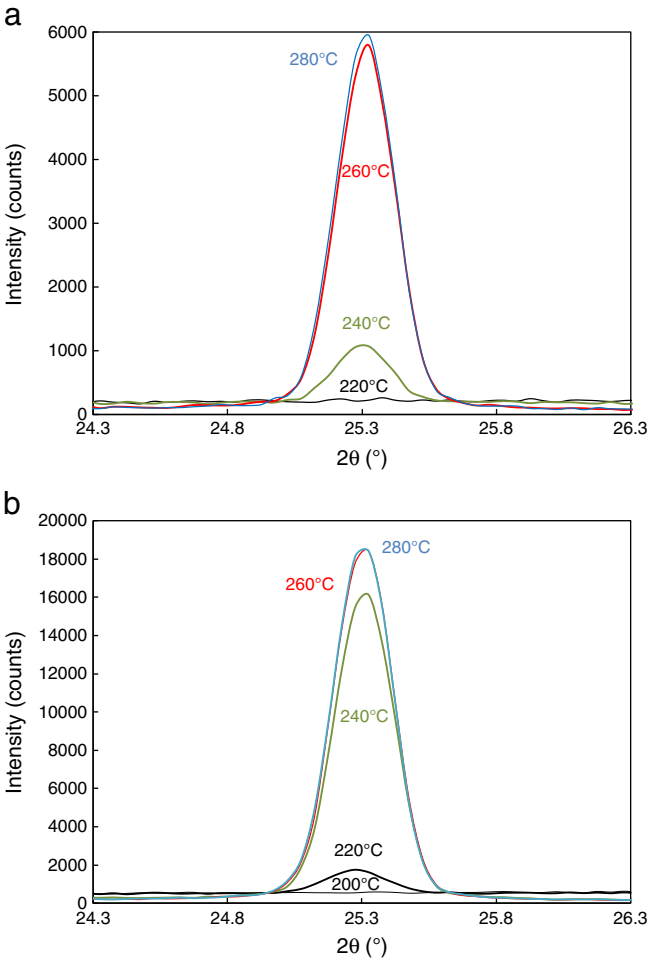

Fig. 1. XRD line profiles of the 101 anatase peak for different temperatures as indicated, for the film of thicknesses 800 nm (a) and 180 nm (b). 200 °C — thin black curve, 220 °C — thick black curve, 240 °C — thick green curve, 260 °C — thick red curve, and 280 °C — thin blue curve.

an ambiguity of the definition of this parameter since it depends also on time. Therefore, we could call it "temperatures of fast crystallization" where the "fast" means here appearance of the diffraction peak within a few minutes. This temperature was found to be 220 °C for the films thicker than 300 nm. However, for thinner films the temperature of fast crystallization increased to 240 °C (180 nm), 260 °C (100 nm) and 280 °C (48 nm), respectively. The important findings were also that the line widths of all the peaks were relatively narrow immediately after peak appearance which indicates that large crystallites of the size higher than about 100 nm were formed quickly. This is very different from the behavior of the as-deposited nanocrystalline films of both rutile and anatase for which the crystallite size remains small (below 10 nm) below 400 °C and increased significantly up to 100 nm only at 800 °C [14].

3.2. Isothermal annealing

For detailed studies of crystallization in dependence on time lower temperatures were used than those of the so-called fast crystallization temperature found in previous experiments. In that case the process still exists but it is much slower, it can be well studied in laboratory conditions and does not require synchrotron radiation. The selected temperature was 180 °C but for the film of a thickness of 48 nm the full crystallization would last weeks and therefore two samples, 48 and 130 nm, were measured at 215 °C.

Integrated intensities of the 101 anatase peak for different film thicknesses are shown on Fig. 2. The intensities were normalized with respect to their maximum value reached for each sample after full crystallization. The solid lines in the figure correspond to theoretical calculations (fits) with the well-known Avrami equation [16,17], sometimes called also Johnson–Mehl–Avrami–Kolmogorov (JMAK) equation [18,19], which is used for description of time dependence of crystalline part $x(t)$ or recrystallized part in the case of recrystallization. Common shape of the equation is the following: $x(t) = 1 - \exp(-kt^n)$, where k is the rate of the process and n is the transformation index related to the dimensionality of the growth and on the kinetic order of nucleation. For 3D growth combined with the first order nucleation n is equal to 4.

However, in the present case, it was necessary to modify the equation by the introduction of the crystallization onset, initial time of crystallization t_0, taken as a time when any significant diffracted intensity appears above background in the position of the expected diffracted peak. The equation $I = 1 - \exp[-k(t - t_0)^n)]$ was then applied to the net integrated intensities I of the diffraction peaks and the crystallization onset was fitted together with the rate k and exponent n. The fits performed on the thicker samples gave a fairly good fits with regression coefficients of 0.999, while for some samples thinner than about 200 nm the regression coefficients dropped to 0.994 and the measured intensities during the early stage of crystallization were found to be slightly above the calculated profile. The fit was not very appropriate for the thinnest film (48 nm) as it can be seen on Fig. 3. Anyway, strong dependence of crystallization process on the film thickness has been confirmed also in these time dependences and it can clearly be seen from the comparison of fitted curves on Fig. 4.

Smooth dependences of the crystallization onset and exponent of the Avrami equation on the film thickness can be seen on Fig. 5. By open symbols the values for films annealed at higher temperature (215 °C) are also shown that, of course, cannot fall on the curves. The value of the exponent slightly increases with the film thickness and it is in the range 2−2.5 that is much lower than for usual 3D growth. According to the phenomenological theory such values can correspond either to disc-like growth + instantaneous nucleation or rod-like growth + random nucleation. The crystallization onset t_0 increases rapidly with the decreasing thickness, while the rate k increases for the thicker films (see inset of Fig. 5). Analysis of intensities of more diffraction peaks is under way but this should not change the above findings. The crystallization process can be more complicated for very thin films when it cannot be well described by

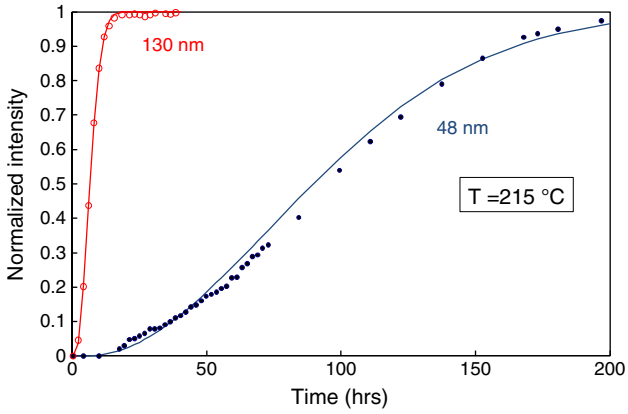

Fig. 3. Dependence of the integrated intensities of anatase diffraction peak 101 normalized to the value reached after crystallization on annealing time for the films of thicknesses 48 and 130 nm, respectively. The symbols represent experimental values, the line is a fitted Avrami equation.

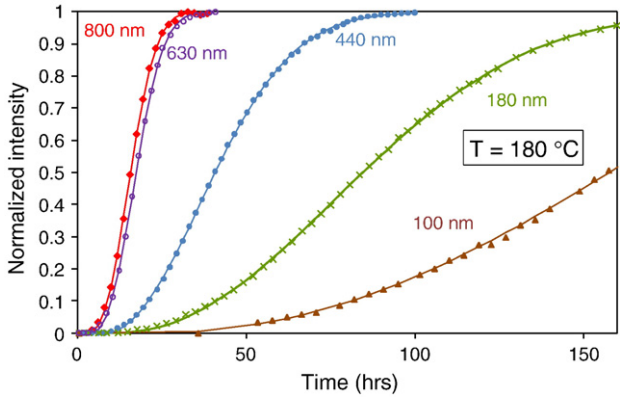

Fig. 2. Dependences of the integrated intensities of anatase diffraction peak 101 normalized to the value reached after crystallization on annealing time for the films with different thicknesses (800 nm — ♦, 440 nm — ●, 180 nm — ×, and 100 nm —▲). The symbols represent experimental values, the lines are fitted Avrami equations with different parameters.

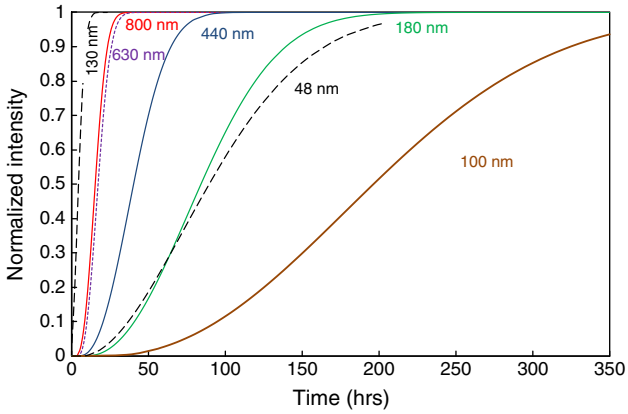

Fig. 4. Full set of dependences of the integrated intensities of anatase diffraction peak 101 calculated from the fitted Avrami equations on the annealing time. Solid lines and dashed line (short lines, for 630 nm) correspond to the films annealed at 180 °C, dashed lines correspond to the films anealed at 215 °C.

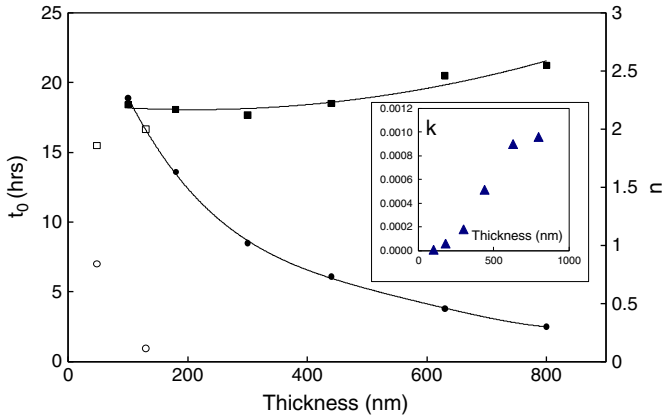

Fig. 5. Dependence of crystallization onset (t_0) (●) and exponent of the Avrami equation n (■) on the film thickness. Filled symbols correspond to the film annealed at 180 °C and open symbols to the films annealed at 215 °C. Lines are added only as a guide for the eye. In the inset, the crystallization rate k is shown.

the JMAK theory. The Avrami exponent can be a function of time. If the dimensionality of the growth is lower than dimensionality of space JMAK behavior is only valid if the orientation of the all growing grains is parallel each other. In other case, blocking of growing grains causes strong deviation from the JMAK theory. The issue has been discussed and modeled recently [20].

3.2.1. Texture variation

XRD peak intensities were varied with the annealing time. Ratios of intensities of two diffraction peaks 101 to 004 are shown on Fig. 6 in dependence on annealing time for several thin films with different thicknesses. While the dependences are not identical for all the films, a clear tendency of an increase of the ratio up to a certain saturation can be seen in all cases. The saturated value of the ratio is usually between 3 and 4 except the thickest film (800 nm) when it goes to 2 and the thinnest film (48 nm) for which it reaches much higher values. Several records for TiO_2 anatase can be found in the ICDD database (see Ref. [21]) with the ratios of 5.4 (calculated for random grain distribution, Rec. no. 89-4921 and 78-2486) and 5.0 (polycrystalline powder, Rec. no. 21-1272). This is somewhat higher than the saturated value here but it must be taken into account that in the present case the measured crystallographic planes are not parallel to the surface in the 2θ scans but inclined by small angles — 13.6° and 17.9° for planes (101) and (001) (the latter measured on diffraction peak 004), respectively. Therefore, the values around 4 correspond roughly to random grain distribution. This agrees well also with previously measured whole diffraction patterns of the films crystallized from the amorphous state — no significant preferred orientation has been found except the very thin films which showed (101) texture. All this means that at the beginning of crystallization the grains oriented with the planes (001) parallel to the surface are preferentially developed but with the proceeding time this preferred orientation is suppressed.

3.2.2. Line broadening

Experimental values of integral breatdhs vs. annealing time for several films are shown on Fig. 7. In general, the line broadening is quite small already from the very beginning of crystallization and does not change significantly with the annealing time. This indicates fast growth of relatively large crystallites already at the beginning of crystallization. Even though the whole physical broadening is ascribed only to the size effect (which is not very realistic) the crystallite size can be estimated to about 100 nm at least, except the thinnest film. The situation is different for the films deposited as nanocrystalline with a crystallite size of 5–10 nm which remained nanocrystalline to relatively high temperatures (600 °C) [14]. This means that it is not possible to prepare nanocrystalline TiO_2 thin films from amorphous ones by annealing, the way that is quite common for preparation of nanocrystalline powders (annealing for specific time at specific temperature for the desired size of nanocrystals).

3.2.3. Peak shifts — stress development

Tensile stresses were found previously in fully crystallized films using a detailed analysis of several peaks on measured post-annealed samples by the conventional $\sin^2\psi$ method. The details of the stress analysis are being described elsewhere [22]. In all cases well linear dependences were observed which correspond well to missing texture and absence of triaxial stresses. Typical plots are shown on Fig. 8 for films with different thicknesses (strong 101 peak, Fig. 8a) showing clear dependence of the slope on film thickness and different peaks measured for the 440 nm film (Fig. 8b) which indicates elastic anisotropy of anatase (see Ref. 22 for more information).

In the present in-situ HT measurements significant shifts of diffraction peaks with the time were observed and tensile residual stresses were confirmed for different diffraction peaks on post-annealed samples measured at room temperature. On Fig. 9 the dependence of interplanar spacing of the (101) plane on annealing time is shown for different films. The lattice spacing is decreasing with the time to some saturated value. This corresponds to the evolution of the stress during annealing and it is well visible in particular for the

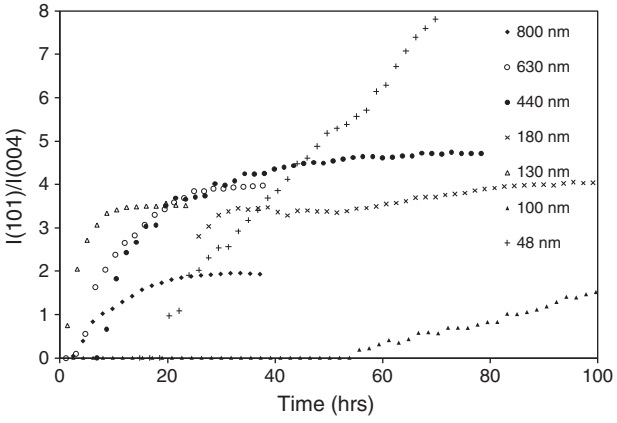

Fig. 6. Ratios of integrated intensities of diffraction peaks 101 and 004 vs. annealing time. Annealing temperatures were 180 °C and 215 °C for the films of thicknesses 800 nm, 630 nm, 440 nm, 180 nm, 100 nm and 130 nm, and 48 nm, respectively.

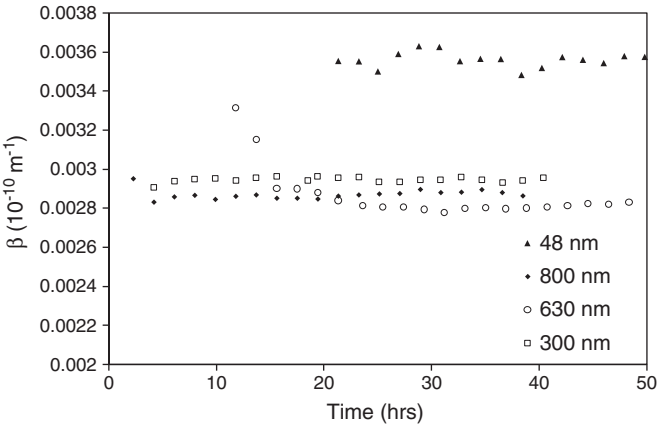

Fig. 7. Measured integral breadth of the 101 anatase peak (in reciprocal space units, $1/d$) vs. annealing time for different film thicknesses. The level of instrumental broadening in the parallel beam geometry was at about 0.0027 (10^{-10} m^{-1}).

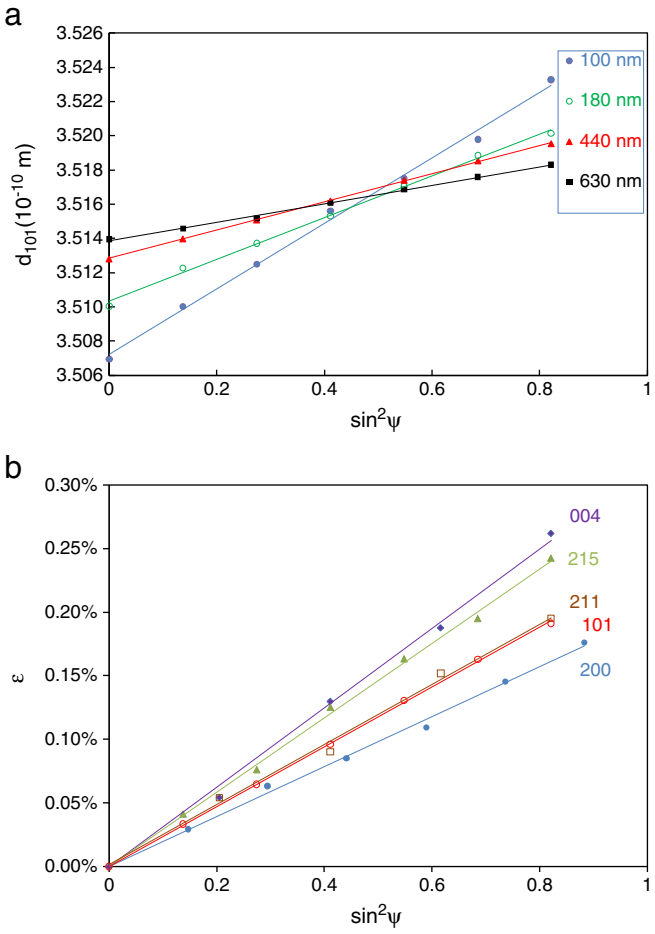

Fig. 8. Typical d vs. $\sin^2\psi$ plots for (101) lattice and different film thickness (a) and lattice strain ε vs. $\sin^2\psi$ calculated for different diffraction peaks and film with a thickness of 440 nm as $\varepsilon_{hkl} = (d_{hkl}(\psi) - d_{hkl}(0))/d_{hkl}(0)$ (b).

thicker films (800, 630 nm), while for thinner films it seems that the stress was formed quite quickly and only the final stage of the process could be observed. For a more detailed analysis, in-situ measurements of more diffraction peaks are necessary and this is under way now. By the $\sin^2\psi$ method applied on the films at room temperature after annealing it was found that the stresses significantly decrease with the increasing film thickness. The results agreed well with the values obtained on these samples by total pattern fitting of 2θ scans [15,22] (Fig. 10). More systematic studies would be required (and are planned) for derivation of more general conclusions, as for example functional type of the dependence and/or extrapolation of the dependence in particular for very small film thickness.

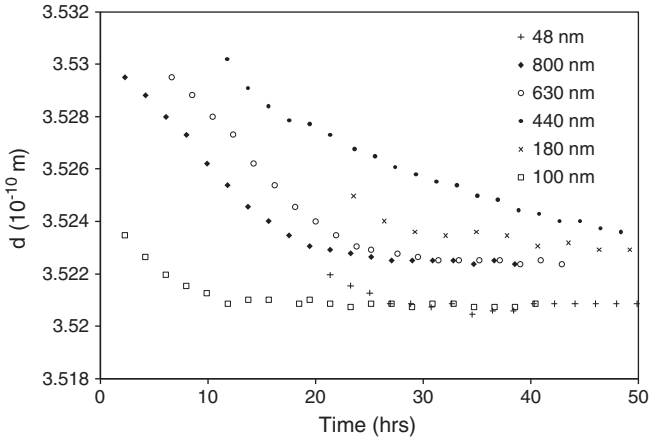

Fig. 9. Changes of lattice spacing d of anatase lattice plane (101) with annealing time for different film thicknesses. Annealing temperatures were 180 °C and 215 °C for the films of thicknesses 800 nm, 630 nm, 440 nm, 180 nm and 130 nm, and 48 nm, respectively.

4. Discussion and conclusions

4.1. Correspondence of the thickness dependence of crystallization to tensile stresses

The results obtained lead to a question what is the reason for such a large thickness dependence of crystallization of titanium dioxide thin films. One reasonable explanation can be related to similar dependence of tensile stresses on the thickness. Such stresses are formed due to the crystallization from the amorphous state because of reduction of specific volume and they are rapidly increasing with decreasing thickness, which is in a good correspondence with the behavior of crystallization. The crystallization onset is plotted against the values of tensile stress on Fig. 11. The dependence is nearly perfectly linear down to the film thickness of 100 nm, which can indicate that the correlation is probable. Similar plot could be constructed for the crystallization rate k but this parameter obtained by the fitting of the Avrami equation is less reliable (because of some correlation of parameters) than the crystallization onset which can also be determined directly. It must also be noted that for the films thinner than about 100 nm, the determination of the residual stress is difficult and less precise because of the weak intensities of diffraction peak analyses and also the JMAK theory is not well valid for these films.

4.2. Summary

By in-situ high-temperature XRD measurements it was confirmed that the speed of crystallization of amorphous TiO_2 thin films is drastically reduced with decreasing film thickness. The time evolution of the integrated intensities of anatase diffraction peaks follow well the Avrami equation modified by the introduction of crystallization onset that increases rapidly with decreasing film thickness. Exception was found only for the films thinner than about 100 nm when the crystallization is more complex and cannot be described by this simple equation. The Avrami exponent is low which can be related to a lower dimension of crystallite growth.

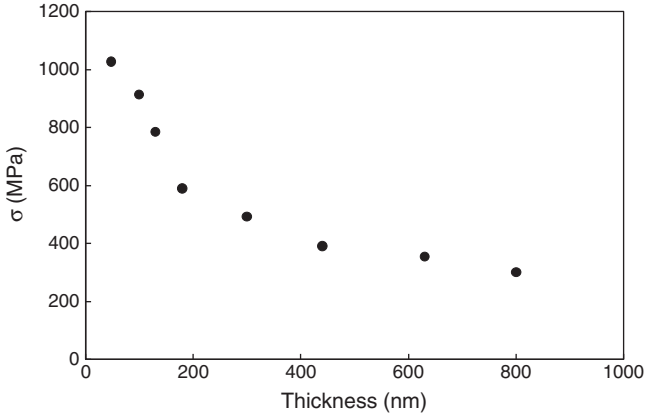

Fig. 10. Dependence of tensile stress determined by the $\sin^2\psi$ method on the film thickness.

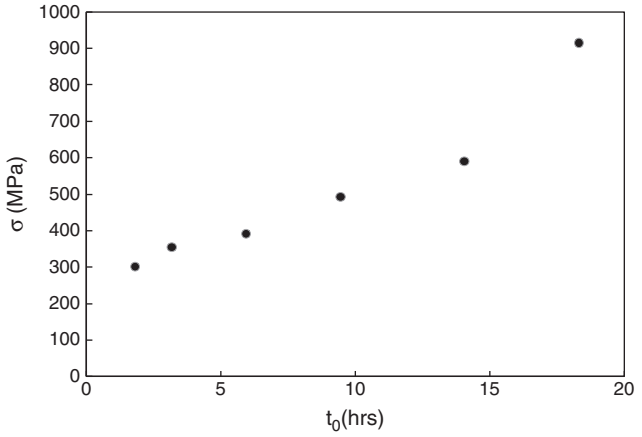

Fig. 11. Relation between the determined tensile stress and crystallization onset.

At the beginning of crystallization the crystallites with (001) orientation are preferentially formed but with annealing time the process results in nearly random distribution of crystallites again with the exception of very thin films for which (101) texture is retained.

The effect of film thickness on crystallization is probably connected to the rapid increase of residual tensile stresses with the decreasing film thickness. The tensile stresses are formed gradually from the beginning of crystallization, as observed from the diffraction peak shifts with the annealing time, and then inhibit the process of crystallization. Anatase crystallites grow quite large quickly already from the beginning of crystallization and therefore the annealing of amorphous film cannot be well used for the preparation of nanocrystalline films.

Acknowledgements

The work is supported by the Grant Agency of the Academy of Sciences of the Czech Republic under numbers KAN40072070 and IAA101120803 and also as a part of the research plan MSM 0021620834 financed by the Ministry of Education of the Czech Republic. The authors are also grateful to Emil Zolotoyabko for useful hints.

References

[1] A. Fujishima, T.N. Rao, D.A. Tryk, J. Photochem. Photobiol. C: Photochemistry Reviews 1 (1) (2000) 1.
[2] S. Banerjeel, J. Gopal, P. Muraleedharan, A.K. Tyagi, B. Raj1, Curr. Sci. 90 (2006).
[3] O. Carp, C.L. Huisman, A., Reller, Prog. Solid State Chem. 32 (2004) 33.
[4] M. Kaneko, I. Okura, Photocatalysis, Science and Technology, Kodansha Ltd., Tokyo, Springer-Verlag Berlin Heidelberg New York, 2002.
[5] L. Gaho, Q. Zhang, Scr. Mater. 44 (2001) 1195.
[6] R. Kužel, L. Nichtová, Z. Matěj, D. Heřman, J. Šícha, J. Musil, Z. Kristallogr. Suppl. 26 (2007) 247.
[7] R. Kužel, L. Nichtová, Z. Matěj, D. Heřman, J. Šícha, J. Musil, 2007, Z. Kristallogr. Suppl. 26 (2007) 241.
[8] Yung-Chiun Her, Yung-Sung Hsu, J. Non-Cryst. Sol. 354 (2008) 3129.
[9] D.Y. Noh, H.H. Lee, T.S. Kang, J.H. Je, Appl. Phys. Let. 72 (1998) 2823.
[10] T.S. Cho, S.J. Doh, J.H. Je, D.Y. Noh, J. Appl. Phys. 86 (1999) 1958.
[11] Wei Xiaoqian, Shi Luping, Chong Tow Chong, Zhao Rong, Lee Hock Koon, Jpn. J. Appl. Phys. 46 (2007) 2211.
[12] C. Zhaom, G. Roebben, M. Heyns, O. Van Der Biest, Key Eng. Mater. 206–213 (2002) 1285.
[13] J. Musil, D. Heřman, J. Šícha, J. Vac. Sci. Technol. A 24 (2006) No.3.
[14] R. Kužel, L. Nichtová, Z. Matěj, J. Šícha, J. Musil, Z. Kristallogr. 27 (2008) 287.
[15] Z. Matěj, R. Kužel, L. Nichtová, Powder Diffr. 25 (2010) 125.
[16] M.J. Avrami, J. Chem. Phys. 7 (1939) 1103.
[17] M.J. Avrami, J. Chem. Phys. 8 (1941) 212.
[18] A.N. Kolmogorov, Izv. Akad. Nauk SSSR, Ser. Mat. 3 (1937) 355.
[19] W.A. Johnson, R. Mehl, Trans AIME 185 (1939) 416.
[20] B.J. Kooi, Phys. Rev. B73 (2006) 054103.
[21] http://www.icdd.com. International Centre for Diffraction Data.
[22] R. Kužel, Z. Matěj, L. Nichtová, Metallurgical and Materials Transactions A (in press).